Available online at www.sciencedirect.com
SCIENCE DIRECT
Journal of Asian Earth Sciences 28 (2006) 363–371
Journal of Asian Earth Sciences
www.elsevier.com/locate/jaes

A tentative 2D thermal model of central India across the Narmada-Son Lineament (NSL)

S.N. Rai *, S. Thiagarajan

National Geophysical Research Institute, Uppal Road, Hyderabad 500 007, India

Received 9 July 2004; received in revised form 10 August 2005; accepted 10 October 2005

Abstract

This work deals with 2D thermal modeling in order to delineate the crustal thermal structure of central India along two Deep Seismic Sounding (DSS) profiles, namely Khajuriakalan–Pulgaon and Ujjan–Mahan, traversing the Narmada-Son-Lineament (NSL) in an almost north–south direction. Knowledge of the crustal structure and P-wave velocity distribution up to the Moho, obtained from DSS studies, has been used for the development of the thermal model. Numerical results reveal that the Moho temperature in this region of central India varies between 500 and 580 °C. The estimated heat flow density value is found to vary between 46 and 49 mW/m^2. The Curie depth varies between 40 and 42 km and is in close agreement with the Curie depth (40 ± 4 km) estimated from the analysis of MAGSAT data. Based on the present work and previous work, it is suggested that the major part of peninsular India consisting of the Wardha–Pranhita Godavari graben/basin, Bastar craton and the adjoining region of the Narmada Son Lineament between profiles I and III towards the north and northwest of the Bastar craton are characterized with a similar mantle heat flow density value equal to ~23 mW/m^2. Variation in surface heat flow density values in these regions are caused by variation in the radioactive heat production and fluid circulation in the upper crustal layer.

Keywords: 2D thermal model; Narmada-Son Lineament; Crustal thermal structure; Curie depth; Moho; Surface heat flow; Heat generation

1. Introduction

Central India is traversed by the ~1600 km long WSW–ENE trending Narmada-Son-Lineament (NSL) which runs from the west coast to beneath the Monghyr–Saharasa ridge and lies between 72–88°E and 21.5–24°N (Eremenko and Negi, 1968). Mishra (1977) has suggested the possible extension of NSL westward into the Arabian Sea and eastward towards the Shillong plateau. It is believed to have originated during the middle to late Archaen (Radhakrishna, 1989). The NSL has influenced the deposition of Neoproterozoic Vindhyan sediments to its north and Gondwana sediments to its south (West, 1962). This central part of India is characterized by the presence of numerous hot springs, feeder dykes for the Deccan traps and appreciable seismicity all along the length of NSL (Krishnaswamy and Ravi Shanker, 1982; Ravi Shanker, 1988; Chandra, 1977; Gahalaut et al., 2004; Rao et al., 2002; Auden, 1949). This region has witnessed Satpura (1938) and Jabalpur (1997) earthquakes of $M > 5$ with the focal depth in the lower crust indicating that the lower crust is of a brittle nature. Because of the significant role of NSL in shaping the tectonic framework of central India, a large number of geological and geophysical studies have been carried out in order to understand the tectonics and evolution of this region (Mukherjee, 1942; Divakara Rao et al., 1998; Verma and Banerjee, 1992; Singh and Meissner, 1995; Roy and Rao, 2000). In this connection, DSS studies have been carried out along five profiles across the NSL in order to delineate the crustal structure of central India (Kumar et al., 2000; Tewari et al., 2001; Sridhar and Tewari, 2001; Mall et al., 2002; Kumar, 2002). These are: (I) Hirapur–Mandla, (II) Khajuriakalan–Pulgaon, (III) Ujjain–Mahan, (IV) Thuadara–Sindad, and (V) Mehamadabad–Billimora. The locations of the first four profiles are shown in Fig. 1. These studies indicate that the Narmada zone was warped, uplifted, rifted and completely buried along the Narmada valley beneath the Deccan volcanic rocks around ~65 Ma. A curvilinear Barvani Sukta Fault (BSF) divides the Narmada zone, the southwestern part representing a graben and northeastern part a basement uplift in the form of a horst structure bounded by two deep seated

* Corresponding author. Tel.: +91 40 23434626; fax: +91 40 27171564.
E-mail address: snrai@ngri.res.in (S.N. Rai).

1367-9120/$ - see front matter © 2005 Elsevier Ltd. All rights reserved.
doi:10.1016/j.jseaes.2005.10.014

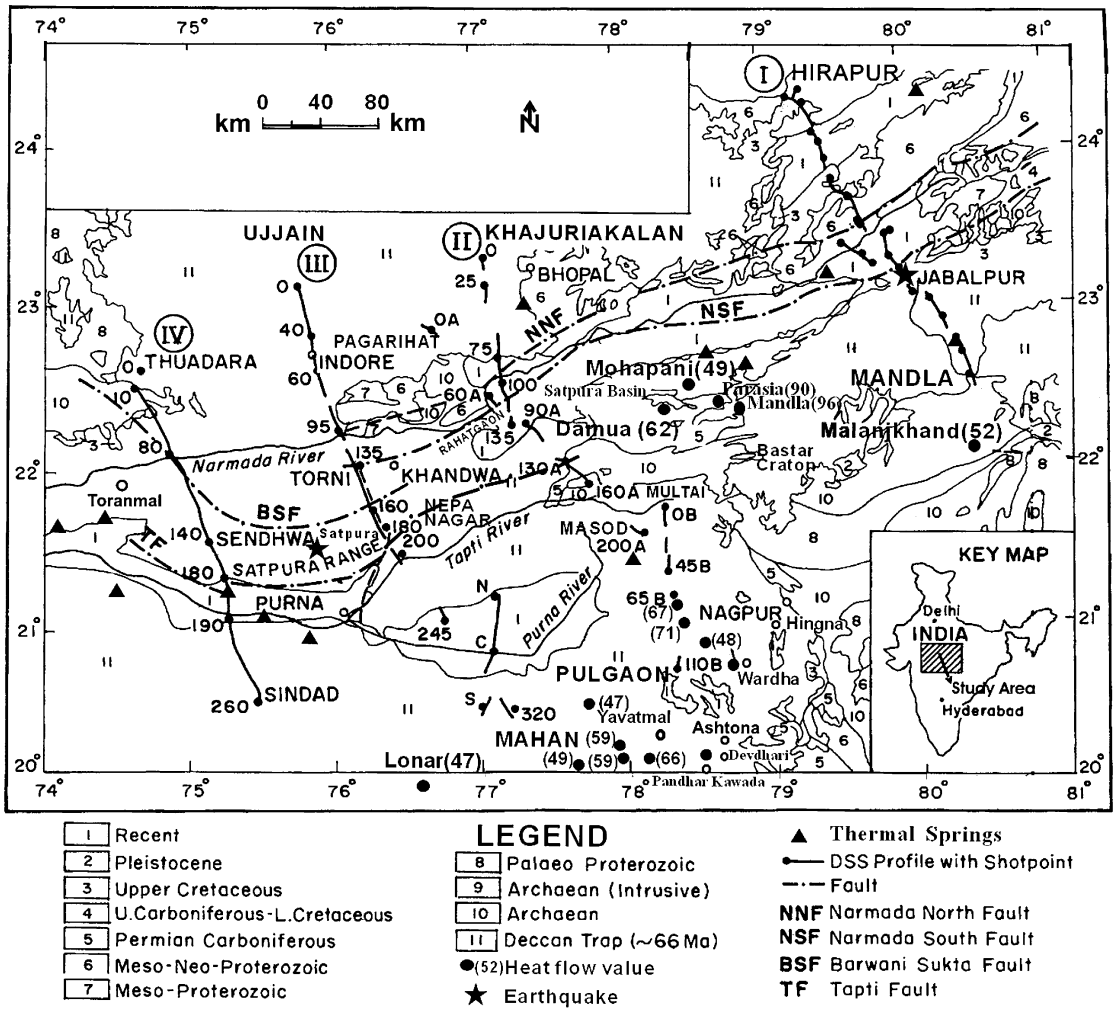

Fig. 1. Geological and Tectonic map of Narmada-Son lineaments with locations of DSS profiles and heat flow sites (modified after Sridhar and Tewari, 2001).

faults which are known as the Narmada North Fault (NNF) and Narmada South Fault (NSF). The last activity along NNF ceased possibly in Permo-Triassic time before the deposition of Upper Jurassic sediments (Jain et al., 1995). Earthquake activities in the vicinity of NNF suggest intermittent slippage. Profiles I, II, III traverse the region of the horst structure while profiles IV and V traverse the graben region almost in a north south direction (Sridhar and Tewari, 2001).

The physical properties of subsurface rocks are affected by variation in the subsurface temperature, which in turn affects most of the geological processes such as lithospheric deformation, earthquake genesis, crustal magnetization etc. Therefore, a knowledge of the subsurface temperature field is essential in order to understand such processes in a region. World-wide, researchers have been using a 2D modeling approach for delineation of the crustal thermal structure along several Deep Seismic Sounding (DSS) profiles. This is because DSS studies provide a 2D crustal structure and P-wave velocity distribution, which are essential in order to carry out 2D thermal modeling. A 2D thermal model was used to compute the temperature–depth distribution along a profile which runs through the Cerro Prieto reservoir, Mexico, by Lippmann and Bodvarsson (1983). Safanda (1985) calculated the 2D temperature distribution along a 250 km long DSS profile in former Czechoslovakia. A 2D thermal structure was estimated along five DSS profiles across major tectonic provinces of Central and Eastern Europe by Cermak (1989). Royer and Danis (1988) have delineated the 2D thermal structure in the region from the Black Forest in Rhinergraben to the southern Vosges. The temperature–depth distribution was calculated along the Taratashskiy profile that crosses the Ural Mountain (Safanda et al., 1992) and along another profile in the central Fennoscandian shield that extends from Archaean granite-greenstone terrain in the NE to the Proterozoic domain in the SW (Kukkonen, 1998). Shengbiao and Jiyang (2000) have computed the temperature field along the 360 km long Wenzhou–Tunxi and 1000 km long eastern segment of the Quanzhou–Heishui orogenic belts in Southeast China. Pasquale et al. (2001) have computed the thermal structure along the 50 km long Alps–Apennines boundary. Shi et al. (2002) calculated the 2D thermal structure of the Xisha Trough, South China Sea. The crustal thermal structure across the Trans European suture zone in the area of the POLONAISE 97 seismic experiment is presented in Majorowicz et al. (2003).

Thiagarajan et al. (2001) presented the crustal thermal structure of the northern Cambay basin along the Tharad–Degam DSS profile. The crustal thermal structure of Godavari graben and the coastal basin along the Paloncha–Narsapur and Kallur–Polavaram DSS profiles is given by Ramana et al. (2003). Rai et al. (2003) published the crustal thermal structure of the NSL region along profile I.

The present work deals with 2D thermal modeling along two DSS profiles, namely the Khajuriakalan–Pulgaon (profile II) and Ujjain–Mahan (profile III), in order to delineate the crustal thermal structure of central India across the NSL. The region under study is surrounded by the Aravalli mobile belt to the northwest, the Bundelkhand craton on the northern side, the Dharwar proto continent to the south and Bastar craton on the southeastern side. For completeness, a brief description of the crustal structure and P-wave velocity distribution along these two profiles, given by Kumar et al. (2000) and Kumar (2002), is presented in the Section 2.

2. Crustal structure and P-wave velocity distribution

The crustal structure and P-wave velocity distribution along profiles II and III are shown in Fig. 2a and b, respectively. The velocity of the exposed Deccan traps is 4.5 km/s. The top layer of 3.7 km/s on profile II and 3.2 km/s on profile III correspond to recent Teritary sediments of the Tapti River. Beneath the Deccan Traps, another layer of 5.2 km/s velocity occurs to the north of NSL. This layer probably represents another flow of the Deccan Traps with higher velocity. The velocity of 5.8–6.1 km/s corresponds to the crystalline basement which is being uplifted between NNF and NSF. The region between NNF and NSF is referred to as the Narmada region. An anomalous high velocity (6.5–6.6 km/s) layer has been observed all along the profile. The depth of this layer is 7–10 km except in the region bounded by NNF and NSF where the depth is ~5 km on profile II and ~2 km on profile III. This layer is thinner within the Narmada region than beyond it. Below this layer, upper crustal velocities of 6.25–6.3 km/s have been observed which is referred to as LVZ in the present study. A velocity of 6.7 km/s is observed for the lower crust. Another velocity jump from 6.7 to 7.2 km/s has been encountered at a depth of ~30 km. The Moho, with a velocity of 8.1 km/s, lies below this layer. The Moho depth for profile II varies between 37 and 42 km while for profile III it varies between 36 and 41 km.

3. Mathematical modeling

The main two sources that contribute to the surface heat flow density value are: (i) heat production within the crust due to decay of unstable isotopes of U, Th, K, and (ii) heat flow density from the mantle. The first one is incorporated in the governing equation as source parameters while the second one is incorporated in the form of a boundary condition. The subsurface temperature field within the crust is estimated by solving the following 2D steady state heat conduction equation

$$\frac{\partial}{\partial X}\left(K\frac{\partial T}{\partial X}\right)+\frac{\partial}{\partial Z}\left(K\frac{\partial T}{\partial Z}\right)=-A(X,Z) \tag{1}$$

subject to the boundary conditions given by

$$T=T_0 \quad \text{at} \quad Z=0 \tag{2}$$

$$\frac{\partial T}{\partial X}=0 \quad \text{at} \quad X=0 \quad \text{and} \quad X=L \tag{3}$$

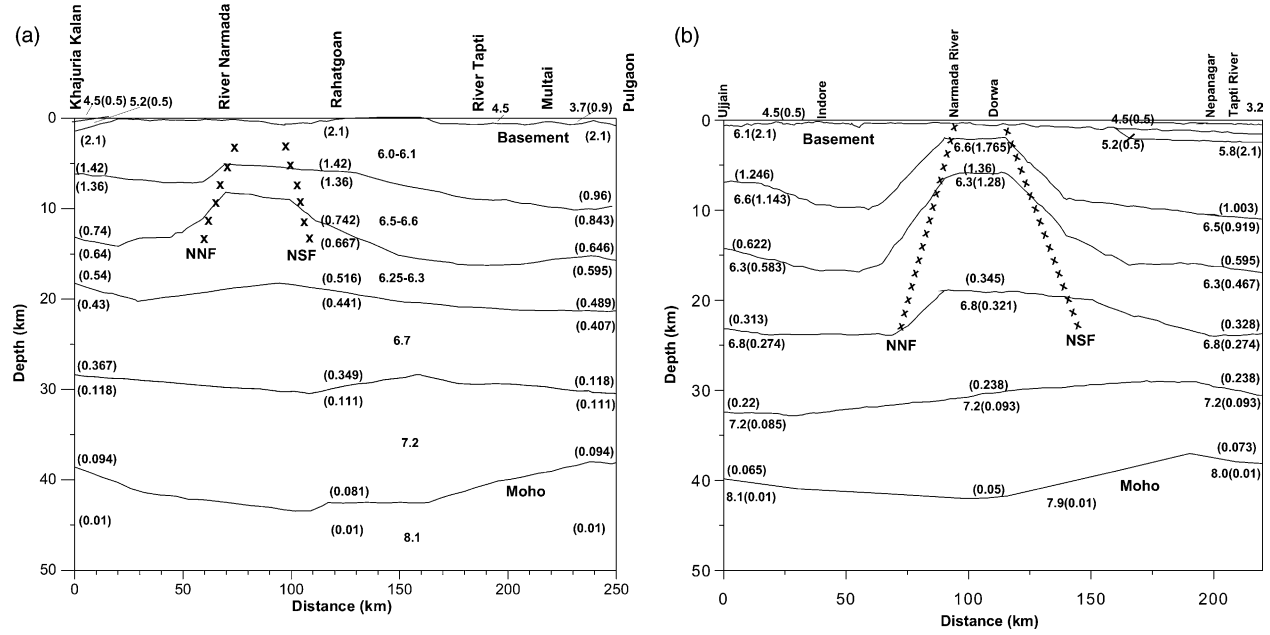

Fig. 2. (a) Crustal layers with V_p—velocity distribution (km/s) and distribution of heat generation (μW/m^3) values (in bracket) along Profile II. Crosses represent the Narmada North Fault (NNF) and Narmada South Fault (NSF); (b) Crustal layers with V_p—velocity distribution (km/s) and distribution of heat generation (μW/m^3) values (in bracket) along profile III. Crosses represent the Narmada North Fault (NNF) and Narmada South Fault (NSF).

$$K\frac{\partial T}{\partial Z} = Q_d \quad \text{at} \quad Z = d \tag{4}$$

in which $T(X, Z)$ is the variable unknown temperature, T_0 is the surface temperature (which is taken as zero for simplicity), $K(X, Z)$ is the thermal conductivity, $A(X, Z)$ is heat production, L and d are the length and depth of the model under consideration, respectively, Q_d is the heat flow density value from the mantle at the base of the model, and X and Z are the orthogonal co-ordinates in horizontal and vertical directions, respectively. The lower boundary of the model is taken below the Moho. In order to solve this boundary value problem for the calculation of temperature distribution, one should know the values of all the controlling parameters such as $A(X, Z)$, $K(X, Z)$, L, d and Q_d appearing in Eqs. (1)–(4).

With precise knowledge of the P-wave velocity distribution available from the DSS studies, the distribution of heat generation A in the middle and lower crustal layer is estimated from the P-wave velocity value by using the following empirical relationship between P-wave seismic velocity (V_p) and radiogenic heat generation (A) for Precambrian rocks (Rybach and Buntebarth, 1984; Cermak, 1989)

$$\ln A = 12.6 - 2.17\, V_p \tag{5}$$

where A is in $\mu W/m^3$ and V_p (20,100) is the velocity (km/s) at room temperature (20 °C) and pressure (100 MPa). The value of A is corrected for 'in situ' pressure and temperature as suggested by Cermak (1989). However, this conversion relationship between V_p and $A(X, Z)$ is not applicable in the upper crustal layer because the upper crust is highly heterogeneous due to the presence of micro cracks that facilitate the redistribution of radioactive elements by groundwater movement. This may have considerably altered the original distribution of the radioactive content of rocks (Cermak, 1989). The heat production in the top layer of volcanic and sedimentary rocks up to the basement is presumed to be constant. For the NSL region, heat production for a sedimentary layer (3.2–3.7 km/s) is taken as equal to 0.9 $\mu W/m^3$ which is the mean of heat production of sandstone, clay and limestone (Rybach and Cermak, 1982). The heat generation value for the Deccan volcanic layer (4.5–5.2 km/s) is taken as 0.47 $\mu W/m^3$, which is the mean of heat generation values estimated from U, Th, K concentrations in the volcanic rocks at 280 and 1100 m depth (Mahoney et al., 2000) using the conversion factor given by Birch (1954).

The heat generation value from the top of basement rocks (5.8–6.0 km/s) to the top of the Low Velocity Zone (LVZ) (6.25–6.3 km/s) is estimated by using an exponential model of radiogenic heat source which is defined by (Lachenbruch, 1970).

$$A(Z) = A_0 \exp\left(\frac{-Z}{D}\right) \tag{6}$$

in which A_0 is the heat production of the basement rock, and D is the logarithmic decrement that represents the thickness of the radioactive enriched crustal layer. In this case $a < Z < b$ km where a is the thickness of the upper layer overlying the basement and b is the depth to the base of the crustal layer above the Low Velocity Zone (LVZ). A_0 and D values for the NSL are not available. However, Gupta et al. (1993) have reported these values for granodiorite from Malanjkhand (22.026°N, 80.715°E) located south of the NSL in the Bastar craton (Fig. 1). These values are: $A_0 = 2.1$ $\mu W/m^3$, $D = 11.5$ km and $K_0 = 3.1$ $Wm^{-1}K^{-1}$. These values for A_0, K_0 and D are used in this study to estimate the heat generation distribution from the top of the basement to the top of the LVZ in the middle crust. The heat generation value for the LVZ is estimated by linear interpolation between the computed value at elements near the upper and lower boundaries of LVZ. Since heat production in the upper mantle is very small, a small value of A equal to 0.01 $\mu W/m^3$ is assigned to the region beneath the Moho (Safanda et al., 1992). The calculated value of A is used within the model area in accordance with the distribution of corresponding V_p velocities. The distribution of estimated heat generation values for profiles II and III are shown within the bracket in Fig. 2a and b, respectively.

In this study, thermal conductivity is considered a function of temperature and is estimated by using the following relation (Cermak and Bodri, 1986; Shengbiao and Jiyang, 2000):

$$K = \frac{K_0}{(1 + CT)} \tag{7}$$

in which K_0 is the thermal conductivity at surface conditions and C is an experimentally determined constant which controls the behaviour of K with temperature T. The values of K_0 and C used in the computation are given in Table 1.

For modeling purposes, the depth of the lower boundary is taken at 50 km which is below the Moho. Gupta et al. (1993) have given a Q_d value equal to 23 mW/m^2 for the Bastar craton and the same value is considered in the present study. With known values of controlling parameters i.e. $K(X, Z)$, $A(X, Z)$, L, d and Q_d, the subsurface temperature distribution is estimated by solving the boundary value problem represented by Eqs. (1)–(4) using a Finite Element based numerical program, named Numerically Integrated System Analysis (NISA). For this purpose, the entire area of the model is divided into a network of four nodes, quadrilateral elements with a 10 km length in the X-direction. Because of the more inhomogeneous character of the upper crustal layer, the region between the ground surface and 10 km depth is divided into relatively smaller elements. The width of the element in the Z-direction is 500 m for the first 10 km and is 2 km below it.

Table 1
Temperature–dependent thermal conductivity values (after Cermak and Bodri (1986))

	K_0 ($Wm^{-1}K^{-1}$)	T (°C)	C (K^{-1})
Upper crust	3.1	<300	0.001
Lower crust	2.0	300–500	0.0
Lithospheric mantle	2.5	>500	−0.00025

4. Numerical results and discussion

4.1. Profile II

The calculated surface heat flow density value and isotherms along profile II are shown in Fig. 3a and b. The numerical results indicate that the Moho temperature varies between 525 and 580 °C. The minimum value is at both ends of the profile while the maximum value is below NSF near Rahatgaon. The heat flow density value varies between 47.3 and 48.2 mW/m^2 with the minimum at NNF near the Narmada River and a maximum at the NSF near Rahatgaon. Approximately

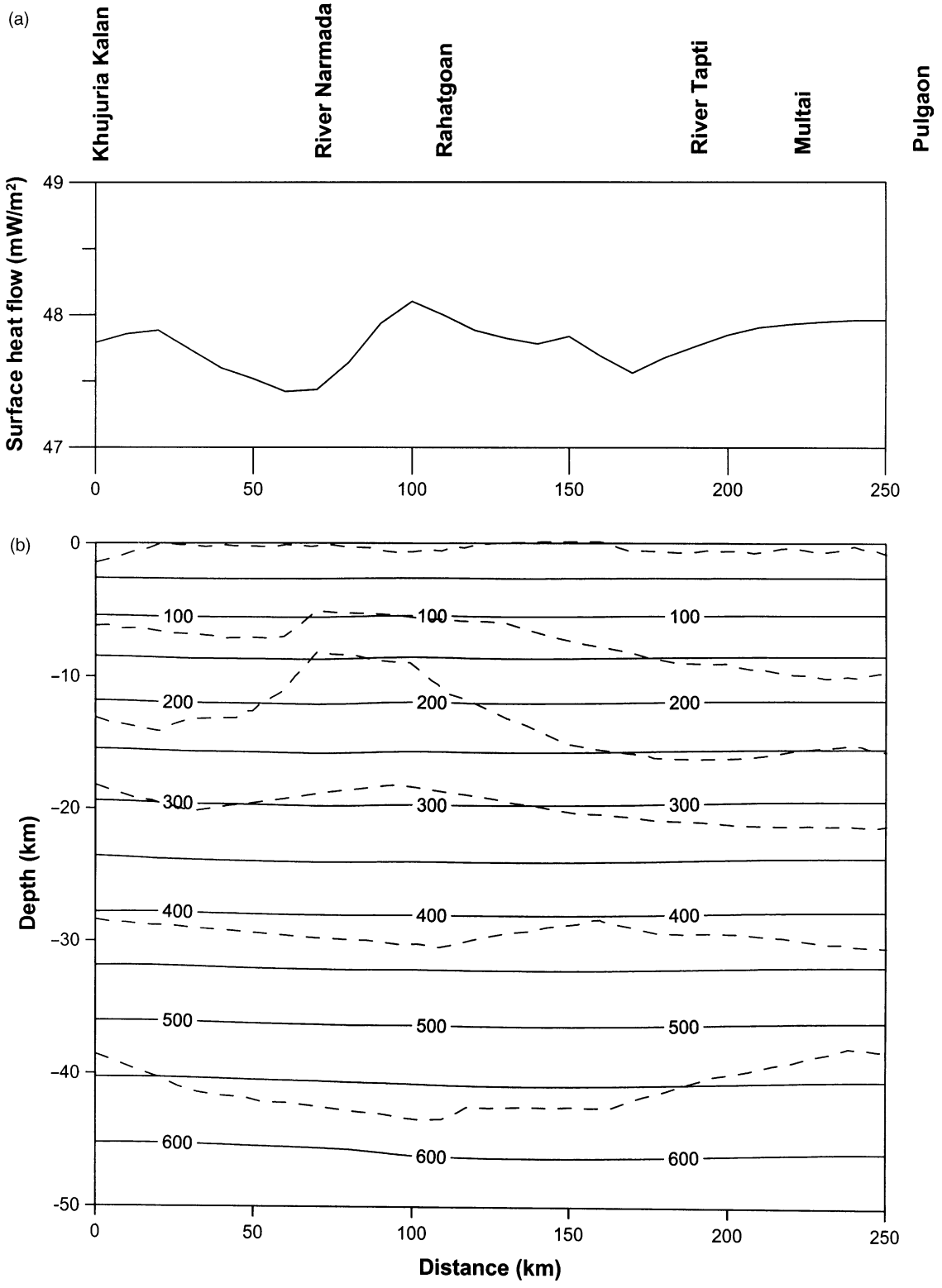

Fig. 3. Calculated (a) surface heat flow density and (b) isotherms (°C) (solid line) along with crustal structure (dotted line) for profile II.

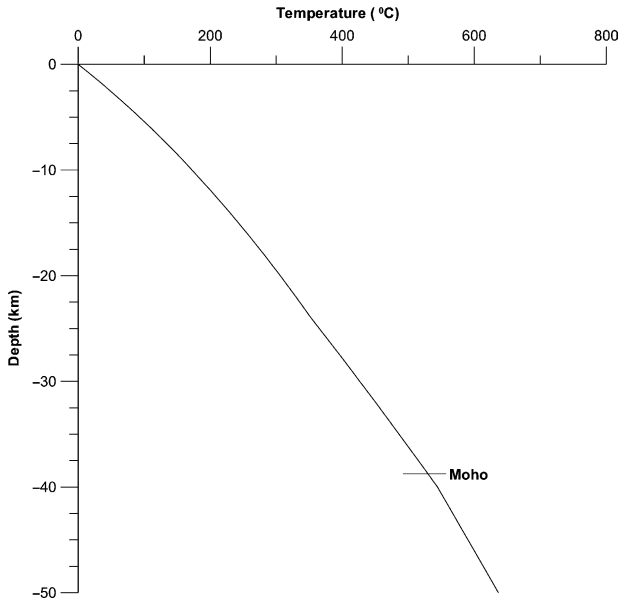

Fig. 4. Calculated temperature–depth distribution at 220 km near Multai on profile II.

~23 mW/m^2 is contributed by the mantle and the remainder is from the crust. These surface heat flow density values are in close agreement with heat flow density values measured at nearby areas such as Lonar (47 mW/m^2), Satephal (47 mW/m^2) and Singdad (49 mW/m^2) in the Yawatmal area, Mandwa (48 mW/m^2) located very near to the Multai–Pulgaon section of the profile in the Wardha area, and Mohapani (49 mW/m^2) located at the northern tips of the Satpura basin south of NSL (Gupta, 1993; Roy and Rao, 2000). The Curie depth, i.e. the depth of the ~550 °C isotherm, is found at 40 km which is 2–3 km below the Moho at both ends and 2–3 km above the Moho in the central region. The calculated temperature gradient near Multai is around 17 °C/km up to 11 km. From below up to the Moho (~38 km), the gradient is around 12.3 °C/km (Fig. 4).

The high surface heat flow density values are also observed at Damua (62 mW/m^2), Parasia (90 mW/m^2) and Mandla (96 mW/m^2) in the Pench Kanhan Valley Coal field located south of NSL in the Satpura basin, Wadhona (71 mW/m^2) and Palora (67 mW/m^2) located very near to the Multai-Pulgoan section of the profile in the Wardha region, and at Dattarampuram (59 mW/m^2), Kurha Talni (66 mW/m^2) and Loni (59 mW/m^2), which are in the region of the NW extension of the Vaidarbha Nadi coalfield in the Yavatmal district as shown in Fig. 1 (Roy and Rao, 2000). Based on geological and geophysical investigations, five major troughs are inferred in the Wardha and Yavatmal regions. Starting from the Nagpur gravity low region towards the south, these troughs are: (i) Kamthi, (ii) Umrer, (iii) Bhander, (iv) Wardha-Pranhita, and (v) Vaidarbha Nadi coal field all extending in a northwesterly direction below the Deccan Traps (Joga Rao et al., 1984; Chary, 1993). The sites of high heat flow density values are associated with gravity lows and resistivity lows indicating the presence of Gondwana sedimentary rocks with fluids and coal seams (Joga Rao et al., 1984; Chary, 1993; Gupta, 1993). This has been confirmed by borehole data drilled near Hingna (79°E 21°5′N) in the Umrer trough and Astona (78°45′E 20°15′N) in the northwesterly extension of the Rajur coal field in the Wardha–Pranhita trough. The presence of hot fluids in the sedimentary rocks may give rise to the high heat flow density value. This fact is supported by the observation of heat flow rise due to hydrothermal circulation across a layer with a 10 °C temperature difference that would contribute about 40 mW/m^2 to the surface heat flow density value (Lachenbruch and Sass, 1977). Towards the southeastern side, these troughs are connected to the probable northward extension of the Pranhita–Godavari Gondwana graben through Wardha and Nagpur and abut the NSL beneath the Satpura basin (Biswas, 2003). The sites of heat flow density values of the order of 49 mW/m^2 and less are located at the boundaries of two adjacent troughs. These boundaries are characterized with less resistivity, indicating that these values are free from the effect of hydrothermal flows and represent the conductive surface heat flow density value for this region in central India. These surface heat flow density values are much less than those suggested by Ravi Shanker (1988) in the range of 70–100 mW/m^2 for the NSL region. His values are mostly in zones of upwelling thermal water and cannot represent the conductive surface heat flow density value. Based on the results of rheological modeling, Manglik and Singh (2002) also suggested that the occurance of deep crustal events at ~35–37 km depth, such as the Jabalpur and Satpura earthquakes, require a surface heat flow density value lower than 48 mW/m^2. There are several other examples of deep earthquakes (25–40 km) such as Saguenay (1988) in east Canada, Soleberg (1938) in Sweden, Manaus (1963) in Brazil and Brome (1979) in Australia that occurred in areas characterized by <50 mW/m^2 heat flow densities (Chen, 1988). Basic dykes and sills associated with the Deccan Traps and several faults such as the Parasia fault exist in the Satpura basin (Gupta, 1993; Datta, 1993; Biswas, 2003). These dykes and faults control water movement in the basin. The dyke, if located towards and down the deep side of the basin, would act as a barrier and assist in the upward flow of deep circulating hot water. Faults also work as conduits for the upward movement of hot water. These processes would result in raising the magnitude of surface heat flow density values at Damua (62 mW/m^2), Parasia (90 mW/m^2) and Mandla (96 mW/m^2) in the Pench Kanhan Valley Coal field of the Satpura basin similar to that reported from Ashwaraopet (104 mW/m^2) and Chintalapudi (92 mW/m^2) in Godavari Valley (Rao et al., 1970; Gupta, 1993).

The importance of subsurface temperature estimates in studies on seismogenesis is essentially in estimating the depth of the brittle–ductile (B–D) transition that represents the depth of seismicity. Experimental results have shown that quartz, feldspar and olivine become ductile at 300, 450 and 700–750 °C, respectively, for natural strain rates (Meissner and Strehleau, 1982; Chen and Molnar, 1983). It is, therefore, possible to arrive at a plausible crustal thermal model of a region by comparing the depth of the B–D transition with focal depth. The numerical results of the present study indicate that the 450 °C isotherm lies at a depth of ~33 km which is the depth of the brittle–ductile transition representing the depth

of seismicity in the lower crust. This is supported by focal depths of ~35 km for the Jabalpur and Satpura earthquakes somewhere in the lower crust (Bhattacharya et al., 1997; Rao et al., 2002; Gahalaut et al., 2004).

4.2. Profile III

The calculated surface heat flow density values and isotherms along profile III are shown in Fig. 5a and b. Numerical results indicate that the Moho temperature varies between 500 and 550 °C, which more or less coincides with the Curie depth. The estimated surface heat flow density values vary between 46.3 and 47.1 mW/m^2 with the maximum near Ujjain and the minimum over the Tapti basin. Approximately 23 mW/m^2 is the contribution from the mantle and the remainder is from within the crust. Although measured heat flow density values in the study area along the profile are not available for comparison, these values are in close agreement

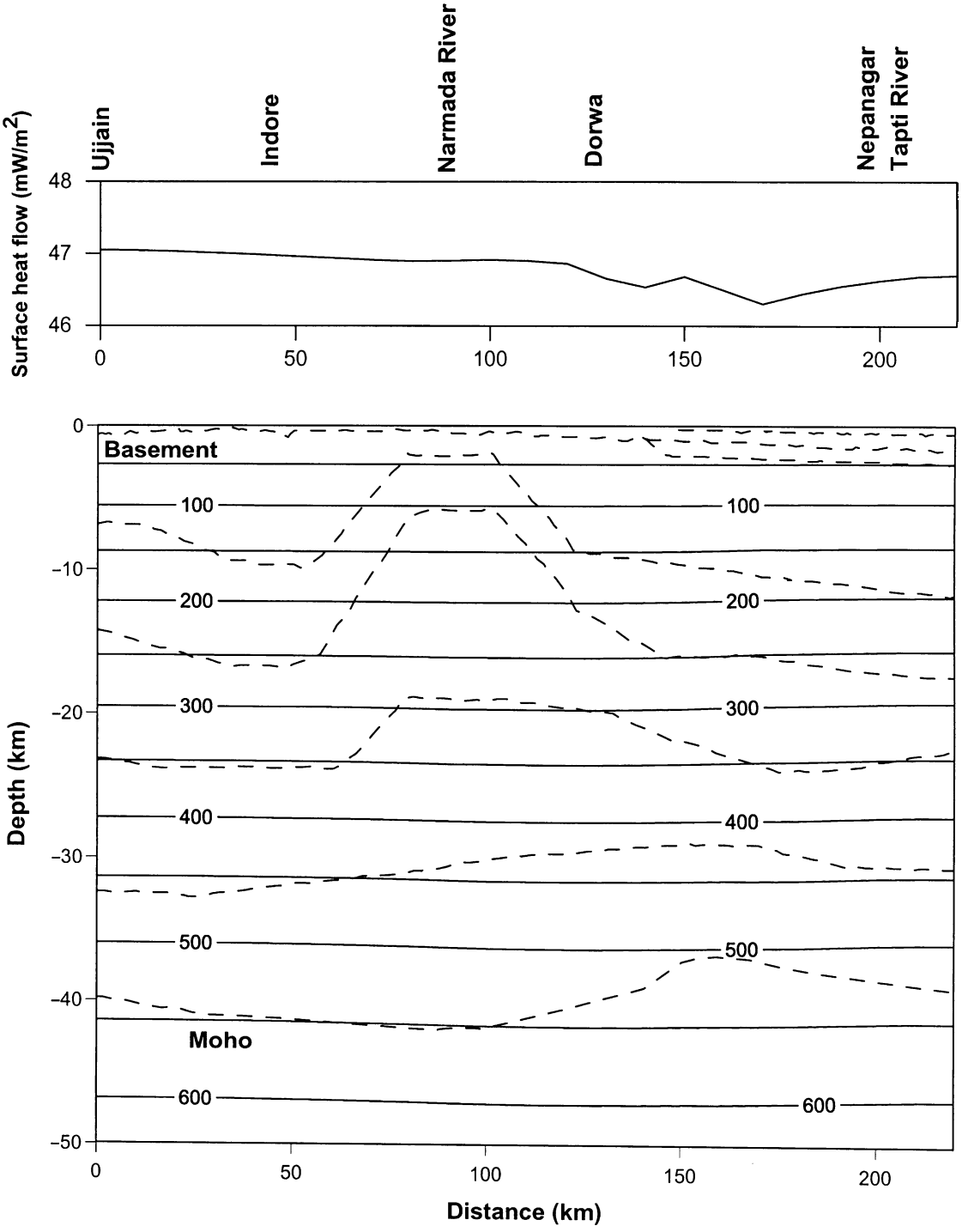

Fig. 5. Calculated (a) surface heat flow density and (b) isotherms (°C) (solid line) along with crustal structure (dotted line) for Profile III.

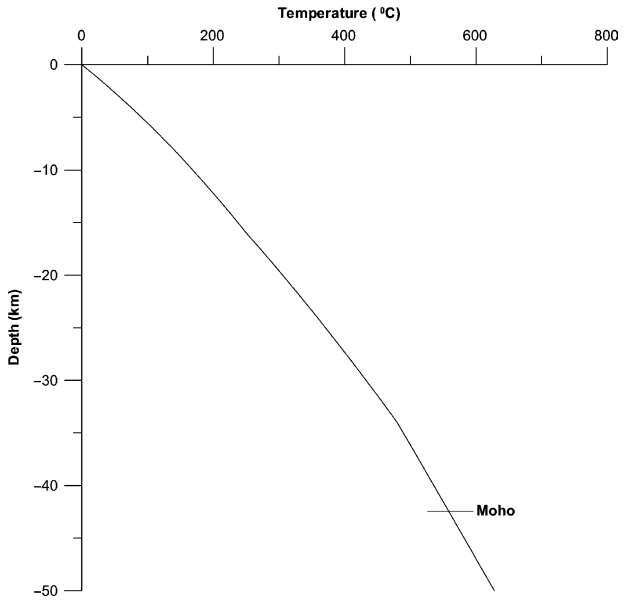

Fig. 6. Calculated temperature–depth distribution at 70 km on Profile III.

with the measured surface heat flow density values at Lonar (47 mW/m^2), Satephal (47 mW/m^2) and Singdad (49 mW/m^2) in the Yawatmal area near Mahan (Gupta, 1993; Roy and Rao, 2000) as shown in Fig. 1. The Curie depth is found at ∼42 km, which more or less coincides with the Moho depth up to the Narmada River and south of Narmada. It is below the Moho with a maximum difference of 5 km in the center of Dorwa and Tapti River.

The calculated temperature–depth profile at 70 km distance near NNF is shown in Fig. 6. The temperature gradient down to 10 km depth is around 16.9 °C/km. Below 10 km depth to the Moho (∼42 km), the grandient is around 12 °C/km.

5. Conclusions

The numerical results indicate that the surface heat flow density value in central India varies between 46 and 49 mW/m^2 and is in close agreement with heat flow density values measured at other places such as Lonar (47 mW/m^2), Satephal (47 mW/m^2) and Singdad (49 mW/m^2) in the Yawatmal area, Mandwa (48 mW/m^2) located near the Multai–Pulgaon section of profile II in Wardha, and Mohapani (49 mW/m^2) located in the northern Satpura basin south of NSL. The Moho temperature varies between 500 and 580 °C, which indicates that the lower crust in this region is cool and brittle, consistent with the depths of deep focused earthquakes such as Satpura (1938) and Jabalpur (1997). The Curie depth is found to vary between 40 and 42 km, which is in close agreement with the Curie depth (40 ± 4 km) given by Agrawal et al. (1992) based on the analysis of MAGSAT data. A similar crustal thermal structure has been reported by Rai et al. (2003) for the central Indian region along the Hirapur-Mandla DSS profile. Based on the present and previous work (Ramana et al., 2003; Gupta et al., 1993), it is suggested that a major part of peninsular India consisting of the Wardha-Pranhita Godavari graben/basin, Bastar craton and adjacent Narmada Son Lineament region between Profiles I and III towards the north and northwest of the Bastar craton are characterized with a similar mantle heat flow density of ∼23 mW/m^2. Variation in surface heat flow density values in these regions are caused by variations in radioactive heat production and groundwater circulation in the upper crustal layer.

Acknowledgements

Authors are grateful to Dr V.P. Dimri, Director, NGRI, for his encouragement and kind permission to publish this work. The suggestions from the reviewers have greatly helped in improving the manuscript. Our thanks are due to Department of Science and Technology for funding the project.

References

Agrawal, P.K., Thakur, N.K., Negi, J.G., 1992. MAGSAT data and curie depth below deccan flood basalts (India). Pageoph 138 (1), 61–75.

Auden, J.B., 1949. Dykes in Western India—a discussion of their relationship with Deccan Traps. Transaction National Institute of Science, India 3, 123–157.

Bhattacharya, S.N., Ghose, A.K., Suresh, G., Baidya, P.R., Saxena, R.C., 1997. Source parameters of Jabalpur earthquake of 22 May 1997. Current Science 73 (10), 855–863.

Birch, F., 1954. Heat from radioactivity. In: Faul, H. (Ed.), Nuclear Geology. Wiley, New York, pp. 148–174.

Biswas, S.K., 2003. Regional tectonic framework of the Pranhintha–Godavari basin. India. Journal of Asian Earth Sciences 21 (6), 543–551.

Cermak, V., 1989. Crustal heat production and mantle heat flow in central and eastern Europe. Tectonophysics 159, 195–215.

Cermak, V., Bodri, L., 1986. Tow-dimensional temperature modeling along five east-European geotraverses. Journal of Geodynamics 5, 133–163.

Chandra, U., 1977. Earthquakes of Peninsular India—a seismotectonic study. Bulletin of Seismological Society of America 67, 1387–1413.

Chary, N.R., 1993. Structure tectonics and basinal history of Vaidarbha Nadi coalfield of Yavatmal district, Maharashtra. Gondwana Geological Magazine Special Volume on Birbal Sahani Centenary National Symposium on Gondwana of India, January 16–17, pp. 247–253.

Chen, W.P., 1988. A brief update on the focal depths of intracontinental earthquakes and their correlations with heat flow and tectonic age. Seismological Research Letters 59 (4), 263–272.

Chen, W.P., Molnar, P., 1983. Focal depth of intracontinental and intraplate earthquakes and their implications for the thermal and mechanical properties of the lithosphere. Journal of Geophysical Research 88, 4183–4214.

Datta, J., 1993. Mohapani Coal field—its structural features, associated igneous bodies and heat effect on coal seams. Gondwana Geological Magazine Special Volume on Birbal Sahani Centenary National Symposium on Gondwana of India, January 16–17, pp. 286–299.

Divakara Rao, V., Gupta, H.K., Gupta, S.B., Mall, M., Mishra, D.C., Murthy, P.R.K., Narayana, B.L., Reddy, P.R., Tewari, H.C., 1998. A geotransect in the central Indian shield, across the Narmada–Son lineament and the central Indian suture. International Geology Review 10, 1021–1037.

Eremenko, N.A., Negi, B.S., 1968. Tectonic Map of India. Oil and Natural Gas Commssion, Dehradun.

Gahalaut, V.K., Rao, V.K., Tewari, H.C., 2004. On the mechanism and source parameters of the deep crustal Jabalpur earthquake, India, of 1997 May 21: constraints from aftershocks and changes in static stress. Geophysical Journal of International 156, 345–351.

Gupta, M.L., 1993. Surface heat flow values in Gondwana grabens of peninsular India: their significance and implications. Gondwana Geological Magazine Special Volume on Birbal Sahani Centenary National Symposium on Gondwana of India, January 16–17, pp. 425–437.

Gupta, M.L., Sundar, A., Sharma, S.R., Singh, S.B., 1993. Heat flow in the Bastar craton, central Indian shield: implications for thermal characteristics of Proterozoic cratons. Physics of the Earth and Planetary Interiors 78, 23–31.

Jain, S.C., Nair, K.K.K., Yaedekar, D.B., 1995. Geology of the Son-Narmada-Tapti lineament zone, geoscientific studies of the Son–Narmada–Tapti lineament zone. Project CRUMANSONATA. Geological Survey of India, 1–154.

Joga Rao, M.V., Sarkar, R.K., Ghatak, T.K., Saha, K., Ghosh, D.C., 1984. Report on the Geophysical Investigations under Deep Geological project for Delineation of Gondwana Sediments Below Deccan Traps in Parts of Yavatmal District Wardha Valley Coal Field Area, Maharashtra, pp. 1–21.

Krishnaswamy, V.S., Ravi Shanker, V., 1982. Scope of development, exploitation and preliminary assessment of geothermal resource potential of India. Records of Geological Survey of India 111 (II), 17–40.

Kukkonen, I.T., 1998. Temperature and heat flow density in a thick cratonic lithosphere: the Sveka transect, Central Fennoscandian shield. Journal of Geodynamics 26 (1), 111–136.

Kumar, P., 2002. Seismic structure of the continental crust in the central Indian region and its tectonic implications. Unpublished PhD Thesis, Osmania University, p. 140.

Kumar, P., Tewari, H.C., Khandekar, G., 2000. An anomalous high-velocity layer at shallow crustal depths in the Narmada zone, India. Geophysical Journal of International 142, 95–107.

Lachenbruch, A.H., 1970. Crustal temperature and heat production: implication of the linear heat flow relationship. Journal of Geophysical Research 75, 3291–3300.

Lachenbruch, A.H., Sass, J.H., 1977. Its nature and physical properties. In: Heacock, J.G. (Ed.), The Earth's Crust Geophysical Monograph, vol. 20, pp. 626–675.

Lippmann, M.J., Bodvarsson, G.S., 1983. Numerical studies of the heat and mass transport in the Cerro Prieto geothermal field, Mexico. Water Resources Research 19 (3), 757–767.

Mahoney, J.J., Sheth, H.C., Chandrasekharam, D., Peng, Z.X., 2000. Geochemistry of Flood Basalts of the Toranmal section, Northern Deccan Traps, India: implications for regional Deccan stratigraphy. Journal of Petrology 41 (7), 1099–1120.

Majorowicz, J.A., Cermak, V., Safanda, J., Krzywiec, P., Wroblewska, M., Guterch, A., Grad, M., 2003. Heat flow models across the trans-European suture zone in the area of the POLONAISE 97 seismic experiment. Physics and Chemistry of the Earth 28, 375–391.

Mall, D.M., Sarkar, D., Reddy, P.R., 2002. Seismic signature of sub-trappean Gondwana basin in central India. Gondwana Research 5, 613–618.

Manglik, A., Singh, R.N., 2002. Thermomechnical structure of the central Indian shield: constrains from deep crustal seismicity. Current Science 82, 1151–1157.

Meissner, R., Strehleau, J., 1982. Limits of stresses in continental crust and their relation to the depth frequency distribution of shallow earthquakes. Tectonics 1, 73–89.

Mishra, D.C., 1977. Possible extension of the Narmada-Son lineament towards Murray ridge (Arabian Sea) and the Eastern Syntaxial bend of the Himalayas. Earth and Planetary Science Letters 36, 301–308.

Mukherjee, S.M., 1942. Seismological features of the Satpura earthquake of the 14th March 1938. Proceeding of the Indian Academy of Science 16, 167–175.

Pasquale, V., Verdoya, M., Chiozzi, P., 2001. Radioactive heat generation and its thermal effects in the Alps–Apennines boundary zone. Tectonophysics 331, 269–283.

Radhakrishna, B.P., 1989. Suspect tectono-stratigraphic terrance elements in the Indian subcontinent. Journal of Geological Society of India 34, 1–24.

Rai, S.N., Thiagarajan, S., Ramana, D.V., 2003. Seismically constrained 2-D thermal model of Central India along Hirapur–Mandla Deep Seismic Sounding profile across the Narmada Son Lineament. Current Science 85 (2), 208–213.

Ramana, D.V., Thiagarajan, S., Rai, S.N., 2003. Crustal thermal structure of the Godavari graben and coastal basin. Current Science 84 (8), 1116–1122.

Rao, R.U.M., Verma, R.K., Rao, G.V., Hamza, V.M., Panda, P.K., Gupta, M.L., 1970. Heat flow studies in the Godavari Valley (India). Tectonophysics 10, 165–181.

Rao, N.P., Tsukuda, T., Kosuga, M., Bhatia, S.C., Suresh, G., 2002. Deep lower crustal earthquakes in central India: inferences from analysis of regional broadband data of the 21 May 1997, Jabalpur earthquake. Geophysical Journal of International 148, 132–138.

Ravi Shanker, V., 1988. Heat flow map of India and discussions on its geological and economic significance. Indian Mineral 42 (2), 89–110.

Roy, S., Rao, R.U.M., 2000. Heat flow in the Indian shield. Journal of Geophysical Research 105 (B11), 25587–25604.

Royer, J.J., Danis, M., 1988. Steady state geothermal model of the crust and the problem of the boundary conditions: application to a rift system, the Southern Rhinegraben. Tectonophysics 156, 239–255.

Rybach, L., Buntebarth, G., 1984. The variation of heat generation, density and seismic velocity with rock type in the continental lithosphere. In: Cermak, V., Rybach, L., Chapman, D.S. (Eds.), Terrestrial Heat Flow Studies and the Structure of the Lithosphere. Tectonophysics 103, 335–344.

Rybach, L., Cermak, V., 1982. Radioactive heat generation in rocks. In: Angenheister, H.G. (Ed.), Properties of Rocks, vol. 1. Springer, Berlin, pp. 353–371.

Safanda, J., 1985. Calculation of temperature distribution in two-dimensional geothermal profile. Studia Geophysica et Geodaetica 29, 191–207.

Safanda, J., Kashubin, S., Cermak, V., 1992. Temperature modelling along the Taratashisky profile crossing the Ural mountains. Studia Geophysica et Geodaetica 36, 349–357.

Shengbiao, H., Jiyang, W., 2000. Heat flow, deep temperature and thermal structure across the orogenic belts in southeast China. Journal of Geodynamics 30, 461–473.

Shi, X., Zhou, Di., Qiu, X., Zhang, Y., 2002. Thermal and rheological structures of the Xisha trough, south China sea. Tectonophysics 351, 285–300.

Singh, A.P., Meissner, R., 1995. Crustal configuration of Narmada–Tapti region (India) from gravity studies. Journal of Geodynamics 20, 111–127.

Sridhar, A.R., Tewari, H.C., 2001. Existence of a sedimentary graben in the western part of Narmada zone: seismic evidence. Journal of Geodynamics 31, 19–31.

Tewari, H.C., Murty, A.S.N., Kumar, P., Sridhar, A.R., 2001. A tectonic model of the Narmada region. Current Science 80 (7), 873–878.

Thiagarajan, S., Ramana, D.V., Rai, S.N., 2001. Seismically constrained two-dimensional crustal thermal structure of the Cambay basin. Proceedings of the Indian Academy of Sciences (Earth and Planetary Science) 110 (1), 1–8.

Verma, R.K., Banerjee, P., 1992. Nature of continental crust along the Narmada Son lineament, inferred gravity and deep seismic sounding data. Tectonophysics 202, 375–397.

West, W.D., 1962. The line of Narmada–Son Valley. Current Science 31, 143–144.